

Variations in Rotational Barriers of Allyl and Benzyl Cations, Anions, and Radicals

Zhe Li,[†] Thomas Bally,^{*,‡} Kendall N. Houk,^{*,†} and Weston Thatcher Borden^{*,§}

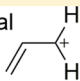
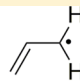
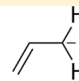
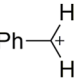
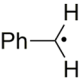
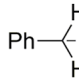
[†]Department of Chemistry and Biochemistry, University of California, Los Angeles, California 90095, United States

[‡]Department of Chemistry, University of Fribourg, Fribourg CH-1700, Switzerland

[§]Department of Chemistry and Center for Advanced Simulations and Modeling, University of North Texas, Denton, Texas 76203-5070, United States

S Supporting Information

ABSTRACT: High accuracy quantum chemical calculations show that the barriers to rotation of a CH₂ group in the allyl cation, radical, and anion are 33, 14, and 21 kcal/mol, respectively. The benzyl cation, radical, and anion have barriers of 45, 11, and 24 kcal/mol, respectively. These barrier heights are related to the magnitude of the delocalization stabilization of each fully conjugated system. This paper addresses the question of why these rotational barriers, which at the Hückel level of theory are independent of the number of nonbonding electrons in allyl and benzyl, are in fact calculated to be factors that are of 2.4 and 4.1 higher in the cations and 1.5 and 1.9 higher in the anions than in the radicals. We also investigate why the barrier to rotation is higher for benzyl than for allyl in the cations and in the anions. Only in the radicals is the barrier for benzyl lower than that for allyl, as Hückel theory predicts should be the case. These fundamental questions in electronic structure theory, which have not been addressed previously, are related to differences in electron–electron repulsions in the conjugated and nonconjugated systems, which depend on the number of nonbonding electrons.

CH ₂ Rotational Barriers			
Hückel	-0.83β	-0.83β	-0.83β
G4 (kcal/mol)	32.6	13.7	21.0
			
Hückel	-0.72β	-0.72β	-0.72β
G4 (kcal/mol)	44.9	11.0	23.8

1. INTRODUCTION

The energies required for conformational changes are quantities of fundamental importance in organic chemistry. Of particular interest are the CH₂ rotational barriers in allyl (A) and benzyl (B) cations, radicals, and anions. As shown in Scheme 1, rotation of a CH₂ group disrupts the conjugation of the fully delocalized species. Consequently, the rotational barriers in allylic and benzylic systems are closely related to the delocalization (or resonance) energies of these species, i.e., the energies required to localize a pair of electrons in the ethylenic π bond of allyl or a sextet of electrons in the π MOs of the benzene ring of benzyl.

Over the years, the rotational barriers and delocalization energies of allylic and benzylic systems have been studied both experimentally¹ and theoretically.² However, we note at the outset that these rotational barriers are predicted by Hückel MO (HMO) theory to be independent of charge. Although we now know that the HMO method, devised by Erich Hückel in 1931, is only a very gross approximation devised to make conceptual application of quantum mechanics possible at a time when no quantitative computations were possible for organic molecules, HMO theory has proven to be extremely valuable for understanding phenomena such as aromaticity and antiaromaticity. In this paper, we address why HMO theory is completely wrong in predicting, even qualitatively, the trends in rotational barriers for allyl and benzyl cations, radicals, and anions.

For example, in HMO theory, the CH₂ rotational barriers in allyl cation (A⁺), anion (A⁻), and radical (A[•]) are all equal to the difference in Hückel energies between the two electrons that occupy the π bonding molecular orbitals (MOs) of allyl and ethylene. This HMO energy difference is $-2(\sqrt{2}-1)\beta = -0.83\beta$. The HMO barriers do not depend on how many electrons occupy the nonbonding π-molecular orbital (NBMO) of allyl at the planar and twisted geometries because, as shown in Figure 1, the Hückel energy of the NBMO is α at both geometries.³

The situation is similar for the benzyl cation (B⁺), anion (B⁻), and radical (B[•]): in each species, the rotational barrier is twice the difference between the Hückel energies of the three filled bonding MOs in planar benzyl and in benzene. This HMO energy difference is -0.72β . In benzyl, as in allyl, the number of electrons occupying the nonbonding MO is irrelevant to the barrier height because the energy of the NBMO also remains α at both geometries.

However, HMO theory makes another prediction. The CH₂ rotational barriers in benzyl are predicted to be $0.72\beta/0.83\beta = 0.87$ times as large as those in allyl. Because the rotational barrier heights in benzyl and allyl are both predicted by HMO theory to be independent of the number of electrons that occupy the NBMOs, the barrier heights in benzyl are

Received: June 26, 2016

Published: October 3, 2016

Scheme 1. CH₂ Rotations in Allyl (A) and Benzyl (B) Cations (* = +), Radicals (* = ●), and Anions (* = -) and A*[‡] and B*[‡] Represent the Transition States for CH₂ Rotations

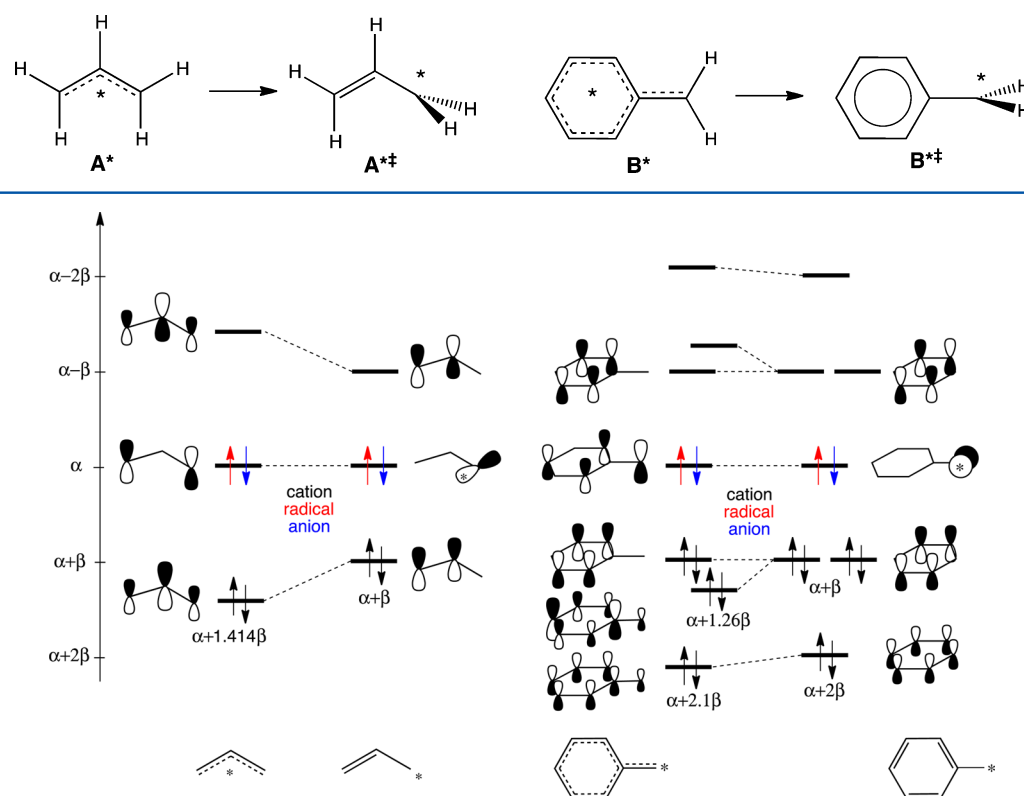


Figure 1. Hückel MOs and MO energies³ of allyl and benzyl cation, radical, and anion at planar geometries and at geometries with a CH₂ group rotated out of conjugation.

expected to be 13% lower than those in allyl in the cations, radicals, and anions.

An early computational study from one of our groups, using the HF/3-21G method, found that HMO theory is incorrect in predicting that the CH₂ rotational barriers are independent of charge. In fact, the barriers to CH₂ rotation computed at this level differ significantly between A⁺ (34.9 kcal/mol), A⁻ (19.0 kcal/mol), and A[•] (14.1 kcal/mol).^{2a} In 1994, Frenking et al. reported that these barriers are 37.8 (A⁺), 23.1 (A⁻), and 12.7 kcal/mol (A[•]), respectively, at the MP2/6-31G(d) level of theory.^{2d} In 1994, Hrovat and Borden calculated a barrier height of 15 kcal/mol for the allyl radical at the CASCI/D+Q/6-31G* level of theory,^{2e} suggesting that the UHF/3-21G barrier height is, in fact, more accurate than that computed by (U)MP2/6-31G(d).⁴

Although quantum mechanical methods have greatly advanced in the past two decades, values of the barrier heights to CH₂ rotation in allyl cation, radical, and anion, computed at levels of theory better than (U)MP2/6-31G*, have not been published. This lacuna prompted us to undertake the high accuracy calculations reported in this manuscript and to explain, based on these trustworthy numbers, why Hückel theory is completely wrong in predicting the sizes of the barriers for the allyl and benzyl cations, radicals, and anions.

Unfortunately, experimental values for the CH₂ rotational barriers of allyl cation, radical, and anion in the gas phase are not available. Nevertheless, some barriers have been measured in solution. For example, the rotational barrier of A⁺ in superacid media was estimated to be 23.7 ± 2 kcal/mol by

extrapolating from experimental barriers of substituted allyl cations.^{1a} The rotational barrier of A[•] was measured by EPR experiments in a mixture of solvents to be 15.7 ± 1.0 kcal/mol.^{1b} The rotational barrier of allyl cesium, the salt of A⁻, in THF was reported to be 18.0 ± 0.3 kcal/mol and declared to be a lower limit for the rotational barrier in free A⁻.^{1c} The relative sizes of these allyl rotational barriers in solution, cation > anion > radical, are consistent with the (U)HF/3-21G barrier heights^{2a} but not with the (U)MP2/6-31G* values.^{2d}

It should be noted that the experimental barriers for A⁺ and A⁻ in solution are expected to be lower than the calculated gas-phase barriers because solvents should selectively stabilize the transition states for CH₂ rotation, where the charge is formally localized on the twisted CH₂ group rather than being delocalized over two carbons in the planar ground states.⁵ Bonding interactions between the allyl ions and their counterions in solution should also make these barriers lower than those computed for the isolated molecules.^{2b} Furthermore, ion-pairing effects will have some influence on these barriers. Theory can establish what are, in principle, upper limits to these very elusive experimental quantities.

The origin of the large apparent variations between the barrier heights to CH₂ rotation in A⁺, A[•], and A⁻ was unknown before our work, but some conjectures have previously been made. For example, the high rotational barrier of A⁺ was attributed to the resonance stabilization of planar A⁺, whereas the resonance stabilization of A⁻ was proposed to be small.^{2b} However, Frenking et al. argued that the delocalization energy of A⁻ is as large as that of A⁺ and

that the barriers in the two ions are higher than that of the radical because of the charge redistribution associated with the conjugation in the planar ground states.^{2d}

Another possible factor to consider is that the nonbonding MO of planar allyl contains an antibonding 1,3- π interaction between the 2p-AOs on the terminal carbons (see Figure 1). The 1,3-antibonding π interaction in the allyl anion probably explains the finding reported by Barbour and Karty that the calculated C–C–C bond angle in allyl anion (132.1°) is much larger than that in the allyl cation (118.8°).⁶ However, this effect would be expected to result in a decrease of the barriers in the order cation > radical > anion, contrary to the results of the (U)HF/3-21G calculations^{2a} and the experiments in solution.

Linares et al. argued that the electronic structures of A⁺ and A⁻ should both be described using the two traditional localized Lewis structures plus a structure with a long π bond between the two terminal carbons, a resonance structure that they claimed does not exist in the allyl radical.^{2h} They viewed this as accounting for the extra stability of planar A⁺ and A⁻ (and hence the higher rotational barriers) compared to A[•]. However, a resonance structure for the allyl anion that has a long π bond between the terminal carbons requires that the nonbonding π MO of allyl be empty and that the two electrons that occupy it in HMO theory be excited into the antibonding π MO in Figure 1.

Very few experimental data are available for the rotational barriers in the benzyl systems. In 1973, Fraenkel et al. reported NMR studies of benzyllithium derivatives; they measured rotational barriers of ~19 kcal/mol.^{1e} However, when Li was replaced by K, the barriers were too high to be measured, which suggests that coordination of the anionic carbon with the metal plays an important role in reducing the barrier height from that in free B⁻. In 1979, Conradi et al. reported an ESR study of benzyl radicals substituted at the exocyclic carbon.^{1d} Alternating line width effects allowed measurement of the rotational barrier for the methyl derivative to be 13.4 ± 1 kcal/mol, i.e., a little less than in the allyl radical.

On the theoretical side, Houk et al. calculated the barriers for B⁺, B[•], and B⁻ to be 45.4, 20.0, and 28.1 kcal/mol, respectively, at the (U)HF/3-21G level, i.e., they were found to be significantly higher than those of the corresponding allyl systems.^{2a} This is the opposite of what is predicted by HMO theory. However, in accordance with both the prediction of HMO theory and with experimental data,^{1b,d} Hrovat and Borden reported calculations at various correlated levels of theory on the barrier to CH₂ rotation in the benzyl radical and concluded that the barrier is 12.5 ± 1.5 kcal/mol, which is ~3 kcal/mol less than that of the allyl radical.^{2e}

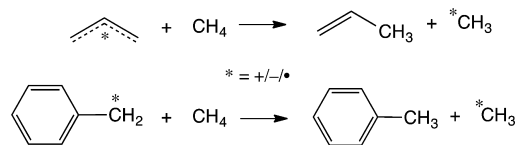
As already noted, the sizes of the rotational barriers in the allyl and benzyl systems are related to the stabilization that a CH₂ group achieves through π -conjugation with a coplanar vinyl or phenyl group, which is replaced by hyperconjugation with σ -MOs upon rotation of the methylene group (see Scheme 1). This stabilization is related to the delocalization energies at the planar geometries. However, delocalization energies vary greatly, depending on choice of the reference system that lacks resonance stabilization. For example, a CH₂ rotational barrier in A[•] or B[•] is not exactly the same as the delocalization energy of planar A[•] or B[•], precisely because upon CH₂ twisting the conjugation with the π MO of ethylene or the π MOs of benzene is replaced by

hyperconjugation with σ MOs of ethenyl or of phenyl. Hyperconjugation in the twisted species makes the barriers to rotation smaller than the conjugation energies lost upon CH₂ rotations.

The literature records vivid debates on the proper way to compute delocalization (or resonance) energies by different quantum chemical methods, such as by imposing constraints on their wave functions or by VB calculations.⁷ Different methods lead to delocalization energies for A⁺ ranging from 22⁶ to 37 kcal/mol^{2d} and all the way to 55 kcal/mol^{2f} (with similar variations for the delocalization energies of A⁻ and A[•]).

One way to eliminate the effect of hyperconjugation on stabilizing the twisted cationic, radical, and anionic allylic and benzylic CH₂ groups is to define the delocalization energies of A[•] and B[•] as shown in Scheme 2. The rotational barriers

Scheme 2. Isodesmic Reactions for Assessing Delocalization Energies



defined in Scheme 1 differ from the reactions in Scheme 2 by transfer of a hydride, hydrogen atom, or proton from methane to the twisted CH₂ group, thus eliminating the contribution of hyperconjugation to the stabilization of the rotated CH₂ group. Therefore, we define the delocalization energies of A[•] and B[•] by the energies of the reactions shown in Scheme 2.

The delocalization energies defined by the isodesmic reactions in Scheme 2 have another advantage over the CH₂ rotational barriers. As already noted, gas-phase rotational barriers have not been measured, and it is not easy to even conceive a method for doing so. However, the gas-phase heats of formation of all of the species in Scheme 2 have been measured, so it is possible to compare the calculated delocalization energies with experimental values.

We have now used high-accuracy quantum chemical methods to recalculate the CH₂ rotational barriers for the allyl and benzyl cations, radicals, and anions, and we have also calculated the delocalization energies of these six species as defined by the energies of the isodesmic reactions in Scheme 2. Herein, we report the results of our calculations, and we identify the major factors that contribute to the surprisingly large differences in rotational barriers and in delocalization energies between the cations, radicals, and anions of both allyl and benzyl.

2. COMPUTATIONAL METHODOLOGY

Calculations were performed with Gaussian09.⁸ All geometries and energies for allyl and benzyl cations, radicals, and anions were calculated by the G4 method.⁹ The B3LYP/6-31G (2df,p) density functional/basis set is used to obtain the geometries in G4. The average absolute deviation of G4 energies from the experiment is reported to be only 0.8 kcal/mol on the G3/05 test set of data.⁹ The energies of allyl systems were also calculated by the W1BD¹⁰ method, which is the Brueckner doubles (BD) variation of Weizmann-1 theory (W1). The root-mean-square deviation of W1BD from the experimental numbers in the G2/97 test set is 0.6 ± 0.5 kcal/mol.¹⁰

B3LYP was also used to calculate the rotational barriers of the allyl and benzyl systems. The results are given in the [Supporting Information](#). They confirmed that the rotational barriers are not very sensitive to the basis sets or to the theoretical methods used to calculate barriers.^{2a} For example, the B3LYP barriers with the 6-311++G** basis set were found to be only slightly higher than those calculated by the WIBD method (by +0.5, +1.2, and +0.9 kcal/mol for A^+ , A^\bullet , and A^- , respectively).

3. RESULTS

3.1. Rotational Barriers of Allyl Cation, Radical, and Anion. The B3LYP/6-31G(2df,p) structures of A^+ , A^\bullet , and A^- and the transition states (marked with a double dagger) for the rotation around a C–C bond are shown in [Figure 2](#).

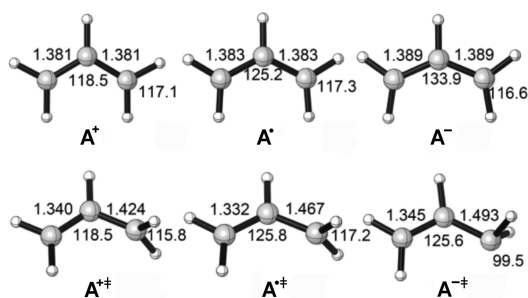


Figure 2. Geometries of A^+ , A^\bullet , and A^- and the transition states for the rotation of their terminal bonds calculated by the (U)B3LYP/6-31G(2df,p) method (bond lengths in Å; bond angles in degrees).

As in previous studies, and in accordance with the expectations from Hückel theory, we found that the C–C bond lengths are quite insensitive to the presence or absence of a charge. However, the C–C–C angle opens on increasing the number of electrons in the a_2 -NBMO of allyl, as expected from the 1,3- π antibonding nature of this MO.⁷ The optimized geometry of allyl anion shows a very small degree of pyramidalization at both terminal carbons.

The geometry differences are more pronounced at the transition states, $A^{+\ddagger}$, $A^{\bullet\ddagger}$, and $A^{-\ddagger}$, for CH_2 rotation, especially with regard to the length of the bond to the rotated carbon. This bond length increases significantly upon going from the cation to the radical and a bit less on going from the radical to the anion.

The twisted CH_2 group is planar in $A^{+\ddagger}$ and $A^{\bullet\ddagger}$ but is pyramidal in $A^{-\ddagger}$. This pyramidalization is consistent with the geometry of the methyl anion¹¹ and with previous calculations on studies of the allyl anion.^{2a,12} Pyramidalization of the twisted CH_2 group in the allyl anion gives rise to two rotational transition states for this species. The one shown in [Figure 2](#) is ~ 2 kcal/mol lower than that of the one where the twisted CH_2 group is pyramidalized in the opposite direction.

Attempted geometry optimization of the transition state for CH_2 rotation in $A^{+\ddagger}$ led to a different structure corresponding to the transfer of a hydride from the central to the rotated carbon. This isomerization reaction forms the 2-propenyl cation, an isomer of A^+ that has been observed by infrared spectroscopy in the gas phase.¹³ When the C–C–C angle in $A^{+\ddagger}$ was fixed at the same value as it was in A^+ , it was possible to locate a constrained transition state for rotation of a methylene group in A^+ . This constrained structure, which is shown in [Figure 2](#), is not a true transition state but rather an approximation to the transition structure for methylene

rotation. This interaction is an extreme form of hyperconjugation!

The barriers to rotation for A^+ , A^\bullet , and A^- , calculated by WIBD (and by G4) are 32.8 (32.6), 14.7 (13.7), and 20.8 (21.0) kcal/mol, respectively. For the allyl radical, the barriers computed by these two methods differ by 1.0 kcal/mol, but for the allyl cation and anion, the barriers are the same to within 0.2 kcal/mol.

3.2. Rotational Barriers of Benzyl Cation, Radical, and Anion. The optimized geometries of the corresponding benzyl species and the transition states for rotation of the CH_2 group are shown in [Figure 3](#). The ground states of B^+ ,

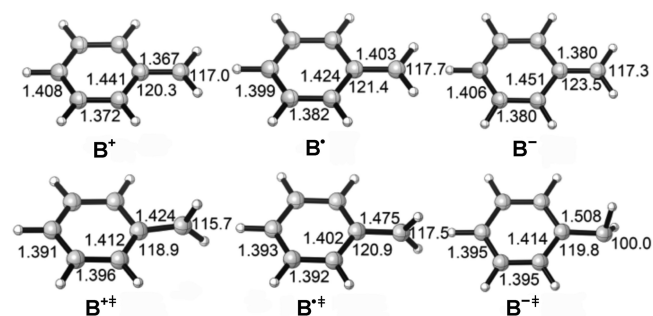


Figure 3. Geometries of B^+ , B^\bullet , and B^- and the transition states for the rotation of their terminal bonds calculated by the (U)B3LYP/6-31G(2df,p) method (bond lengths in Å; bond angles in degrees).

B^\bullet , and B^- are all planar. As in the case of the allyl systems, the bond lengths of the planar species change very little with the number of electrons in the benzylic NBMO with the exception of the exocyclic C–C bond, which is significantly longer in the radical B^\bullet than in the ions B^+ and B^- . The length of this bond in the transition structures also varies much more than the other C–C bond lengths. As in allyl, the exocyclic C–C bond in benzyl is much shorter in $B^{+\ddagger}$ than in $B^{-\ddagger}$ and is intermediate in length in $B^{\bullet\ddagger}$. Furthermore, in $B^{+\ddagger}$, the carbon framework is no longer planar, and the dihedral angle between the methylene C–C bond and the phenyl plane is 11.8° . In $B^{-\ddagger}$, the methylene group is pyramidal, similar to the case $A^{-\ddagger}$.

The WIBD method is too costly to use to calculate the rotational barriers of the $C_6H_5CH_2$ species with our current computing resources. The barriers predicted by the G4 method are 44.9 for B^+ , 11.0 for B^\bullet , and 23.8 kcal/mol for B^- , respectively. The trend of the barriers, i.e., cation > anion > radical, is the same as that in the corresponding allylic systems, and perhaps surprisingly, the numbers are quite consistent with those from the 3-21G calculations that were published almost 30 years ago.^{2a} Although B^+ has a significantly higher barrier than A^+ , the difference between B^- and A^- is smaller, and the barrier is actually slightly larger for A^\bullet than for B^\bullet , in agreement with the calculations of Hrovat and Borden and with the prediction of HMO theory.^{2c}

3.3. Delocalization Energies. We have also computed the delocalization energies of all of the allyl and benzyl species by evaluating the enthalpy changes for the isodesmic reactions shown in [Scheme 2](#). As already discussed, the calculated delocalization energies can be compared unambiguously to values that can be obtained from experimental enthalpies of formation. The calculated and experimental reaction enthalpies are listed in [Table 1](#) along with the calculated G4 rotational barriers.

Table 1. Isodesmic Reaction Enthalpies ($\Delta_r H$) and Rotational Barriers ($\Delta_{\text{rot}} H^\ddagger$) in kcal/mol

species	$\Delta_r H$ (G4)	$\Delta_r H$ (exp) ^a	$\Delta_{\text{rot}} H^\ddagger$ (G4)
A ⁺	57.1	56.74 ± 0.23	32.1
A [•]	18.7	17.50 ± 0.23	13.8
A ⁻	29.7	27.05 ± 0.53	19.7
B ⁺	73.4	75.3 ± 1.7	45.3
B [•]	14.7	15.4 ± 1.5	10.9
B ⁻	36.5	34.6 ± 2.4	23.3

^aFrom data on the active thermochemical tables¹⁴ for the allyl system and from the NIST Webbook¹⁵ for the benzyl system (see Supporting Information).

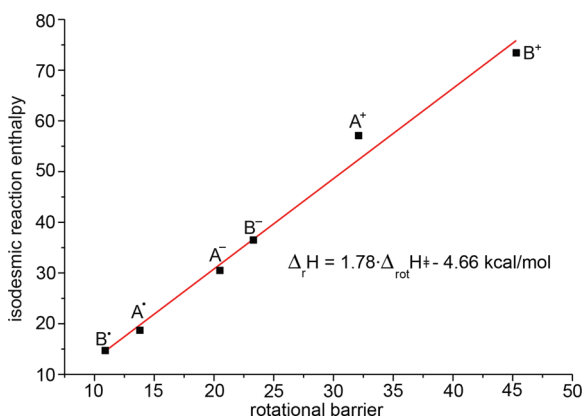


Figure 4. Plot of isodesmic reaction enthalpies vs rotational activation enthalpies (both calculated by the G4 method; $R^2 = 0.988$).

The mean unsigned average deviation of the calculated from experimental isodesmic reaction enthalpies is 1.85 kcal/mol. The largest error is 3.5 kcal/mol for the allyl anion where the experimental uncertainty is quite large. The complete thermochemical data are given in the Supporting Information.

The barriers to rotation are smaller than the delocalization energies from the isodesmic reactions because of the hyperconjugative stabilization at the twisted geometries. Nevertheless, as shown in Figure 4, there is a good correlation between the calculated isodesmic reaction energies and the calculated rotational activation enthalpies.

The energy differences, $\Delta_r H$ (G4) – $\Delta_{\text{rot}} H^\ddagger$ (G4), are largest for the cations (allyl = 25.0 kcal/mol and benzyl = 28.1 kcal/mol), smaller for the anions (allyl = 10.0 kcal/mol and benzyl = 13.2 kcal/mol), and smallest for the radicals (allyl = 4.9 kcal/mol and benzyl = 3.8 kcal/mol). The relative sizes of these differences are consistent with the expectations that hyperconjugation should have the largest stabilizing effects on the twisted CH_2 groups in the allyl and benzyl cations, smaller stabilizing effects in the allyl and benzyl anions because of the pyramidalization of the twisted CH_2 group, and the smallest stabilizing effects in the allyl and benzyl radicals.

4. DISCUSSION

Table 1 shows that the barrier to CH_2 rotation in the allyl cation is 1.6 times that in allyl anion and 2.3 times that in allyl radical. In benzyl, the barrier to rotation in the cation is 1.9 times that in the anion and 4.2 times that in the radical. Clearly, the barriers to CH_2 rotation in allyl and in benzyl

depend critically on whether the NBMO is occupied by zero, one, or two electrons, a result that is very different from the HMO prediction.

It is well-known that a major flaw in Hückel theory is its failure to explicitly account for the Coulombic repulsion between electrons. Therefore, the reason why the calculated rotational barriers and delocalization energies in Table 1 are different for the cations, radicals, and anions is likely to be due to the effects of electron repulsion terms that are neglected by HMO theory.

Allyl Cation, Radical, and Anion. In discussing the role of electron repulsion on the barrier heights, we first focus on the allyl systems. For simplicity, we begin by assuming that the geometries and all of the orbitals of the allyl cation, radical, and anion, are the same in the planar species. We make the same assumption about the transition states for rotation of a CH_2 group. This is of course not exactly the case, but in the Supporting Information (p. S8) we discuss the effects that result from the differences that we ignored.

In the planar allyl cation, radical, and anion, one pair of electrons occupies π_1 , the bonding π MO of allyl. At the geometry in which the CH_2 group is rotated out of conjugation, the same pair of electrons occupies the bonding π MO of ethylene. In the allyl radical and anion, we must also include one or two electrons in π_2 , the allylic NBMO. In the twisted structure, these electrons occupy the in-plane $2p\text{-AO}$, p_{ip} of the CH_2 group (see Figure 1, left side).

We assume that the Coulomb repulsion between the two electrons in the π_1 bonding MO of planar allyl (which we will call J_{11}^{pl}) is the same in all three planar species, as is the Coulomb repulsion between the two electrons in the ethylenic π MO of the twisted structures (J_{11}^{tw}). However, the ethylenic bonding π MO in the twisted structure is delocalized over one less carbon atom than that of the allylic bonding π MO in the planar structure. Hence, $J_{11}^{\text{tw}} > J_{11}^{\text{pl}}$. This increase in electron repulsion serves to increase the rotational barrier height, relative to the HMO barrier, by a similar amount in all three allyl systems.

For explaining why the rotational barrier in A[•] is less than that in A⁺, the Coulombic repulsion between the unpaired electron and the pair of electrons in the bonding π MOs of planar and twisted allyl must also be considered. The Coulombic repulsion between the electron in the π_2 NBMO of planar allyl and the pair of electrons in the bonding π_1 MO is $2J_{12}^{\text{pl}} - K_{12}^{\text{pl}}$. The exchange integral K_{12}^{pl} corrects for the fact that the unpaired electron has the same spin as one of the electrons in the bonding π MO, and therefore, these two electrons cannot simultaneously occupy the same $2p\text{-}\pi$ AO.¹⁶

In the twisted radical, the term $2J_{12}^{\text{pl}} - K_{12}^{\text{pl}}$ in the planar structure is replaced by $2J_{12}^{\text{tw}} - K_{12}^{\text{tw}}$ for the Coulombic repulsion between the unpaired electron in the in-plane $2p\text{-AO}$ and the pair of electrons in the ethylenic π MO in the twisted structure. However, $2J_{12}^{\text{tw}} - K_{12}^{\text{tw}} < 2J_{12}^{\text{pl}} - K_{12}^{\text{pl}}$ because in the twisted structure the nonbonding electron and the bonding electrons are confined to different regions of space. This qualitatively explains why the barrier to rotation in A[•] is smaller than that in A⁺. Although the one-electron energy of the nonbonding orbital (α in Hückel theory) does not change upon CH_2 rotation, the repulsion between the electron in the nonbonding MO and the pair of electrons in the bonding π MO decreases.

In planar A⁻, there are two electrons in the π_2 NBMO. Therefore, the Coulombic repulsion between the nonbonding

and bonding electrons in the planar anion, $2(2J_{12}^{\text{pl}} - K_{12}^{\text{pl}})$, is twice as large as in the radical. However, in A^- , the pair of electrons in the nonbonding MO also repel each other, and this repulsion contributes J_{22}^{pl} to the Coulombic repulsion in the planar anion.

In the twisted allyl anion, these two nonbonding electrons are both localized in the in-plane 2p AO, where their mutual Coulombic repulsion J_{22}^{tw} is *much* higher than the Coulombic repulsion between the two electrons in the delocalized nonbonding π MO of the planar allyl anion. This difference in the Coulombic interactions between the electrons in the anion and in the radical explains why the rotational barrier of A^- is higher than that of A^\bullet .

The equations for the contributions of the changes in electron repulsion energies (Δ_{elrep}) to the barriers to rotation in the cation, radical, and anion are as follows

$$\text{allyl cation: } \Delta_{\text{elrep}}(\text{A}^+) = [J_{11}^{\text{tw}} - J_{11}^{\text{pl}}] \quad (1)$$

$$\begin{aligned} \text{allyl radical: } \Delta_{\text{elrep}}(\text{A}^\bullet) \\ = [J_{11}^{\text{tw}} - J_{11}^{\text{pl}}] + 2 \cdot [J_{12}^{\text{tw}} - J_{12}^{\text{pl}}] - [K_{12}^{\text{tw}} - K_{12}^{\text{pl}}] \end{aligned} \quad (2)$$

$$\begin{aligned} \text{allyl anion: } \Delta_{\text{elrep}}(\text{A}^-) \\ = [J_{11}^{\text{tw}} - J_{11}^{\text{pl}}] + 4[J_{12}^{\text{tw}} - J_{12}^{\text{pl}}] - 2 \cdot [K_{12}^{\text{tw}} - K_{12}^{\text{pl}}] \\ + [J_{22}^{\text{tw}} - J_{22}^{\text{pl}}] \end{aligned} \quad (3)$$

To quantify the above effects of electron repulsion, we need values for the different Coulomb (J) and exchange (K) integrals that appear in eqs 1–3. For simplicity, we use Pariser–Parr–Pople (PPP) theory¹⁷ to evaluate these integrals.

The results of these PPP calculations are given in the Supporting Information (SI) for this manuscript. As discussed in the SI, because of the approximations that we made in these model calculations, the PPP rotational barriers are not close to the G4 values in Table 1. Nevertheless, the simple PPP model has the virtue of revealing qualitatively why the allyl cation is calculated to have a higher barrier to rotation than the anion and why the anion has a higher barrier than the radical.

The PPP calculations confirm that (a) the Coulombic repulsion (J_{11}) between the pair of electrons in the bonding MO is higher in the more localized ethylenic bonding π MO in the twisted geometry, and this tends to favor the planar geometry for A^+ , A^\bullet , and A^- . (b) In A^\bullet , the Coulombic repulsion between this pair of electrons and the electron in the NBMO ($2J_{12} - K_{12}$) is far smaller in the twisted geometry, where the unpaired electron is localized on the twisted CH_2 group. This localization favors the twisted geometry not only in A^\bullet but also in A^- . (c) However, in A^- , both nonbonding electrons become localized in the AO on the twisted carbon, and their mutual Coulombic repulsion destabilizes the twisted geometry.

Benzyl Cation, Radical, and Anion. Table 1 shows that the ordering of the rotational barriers in the benzyl is qualitatively similar to that in the allyl systems, i.e., cation > anion > radical. The reason for the similarity is that the Coulombic electron repulsion energies change in the same way upon rotation of the CH_2 group in benzyl as they do in allyl and for reasons analogous to those discussed in the preceding section. Of course, in the twisted structure for

benzyl, instead of two electrons being localized in the π bond of ethene, six electrons are localized in the π MOs of a benzene ring.

Despite these similarities between allyl and benzyl, there are also differences. Table 1 shows that the rotational barrier of the benzyl radical is $\sim 20\%$ lower than that of the allyl radical. This is in qualitative accordance with the HMO prediction of a decrease of 14%, as mentioned in the Introduction. However, opposite to the predictions of HMO theory, the rotational barrier in the benzyl anion is computed to be 18% *higher* than in the allyl anion, and in the cations, the barrier increases by over 40% on going from allyl to benzyl!

Why are the rotational barriers in benzyl cation and anion calculated to be substantially higher than those in their allyl counterparts, not lower, as predicted by HMO theory? A clue to the answer is given by comparison of the C– CH_2 bond lengths in Figures 2 and 3. In the three planar allyl systems, these bond lengths are all nearly the same, whereas in the planar benzyl systems, the C– CH_2 bond lengths in the anion and cation are significantly shorter than that in the radical.

This comparison suggests that Coulombic effects, which are neglected in HMO theory, create some π bonding to the exocyclic CH_2 group in the benzyl cation and anion, whereas they do not have this type of effect on increasing π bonding in the allyl cation and anion. This hypothesis would explain why the rotational barrier in the benzyl cation is 40% higher than in the allyl cation and why the rotational barrier in the benzyl anion is 18% higher than in the allyl anion.

For the reasons explained below, in the benzyl cation, radical, and anion, the SCF MOs differ substantially from the HMOs. Therefore, unlike the case in allyl, where we were able to use the HMOs to do a simple and transparent analysis of the changes in electron repulsion that cause the differences in rotational barriers, this is not possible in benzyl. In the paragraphs below, we describe why electron repulsion causes the SCF MOs for benzyl to be rather different from the HMOs.

It is easy to understand why the optimal orbitals for the planar benzyl cation are quite different from the HMOs. In Hückel theory, the charge on the exocyclic CH_2 group in planar benzyl cation is $+4/7$; thus, this carbon provides a site of comparatively low electron density (and hence low potential energy) to which electron density can delocalize from the phenyl π system. This delocalization can be described as involving mixing predominantly between the highest occupied HMO ($2b_1$) that has the same symmetry as the empty nonbonding HMO ($3b_1$). These two Hückel MOs and the resulting SCF MO are depicted in Figure 5.

If the phases of the 2p-AO at the exocyclic carbon are chosen to be the same in the $2b_1$ and $3b_1$ MOs, the phases at

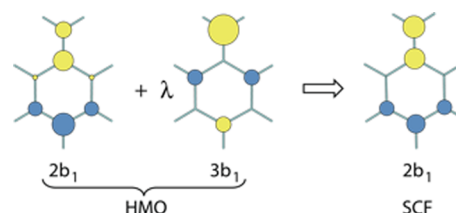


Figure 5. Schematic depiction of the $2b_1$ ($E = \alpha + 1.26\beta$) and the $3b_1$ ($E = \alpha$) HMOs of benzyl and the doubly occupied $2b_1$ SCF MO of the cation that results from mixing a small amount ($\lambda < 1$) of the latter HMO into the former HMO.

the *ortho*- and *para*-carbons in these MOs are the opposite. This means that the mixing of the empty $3b_1$ MO into the filled $2b_1$ MO with a positive sign has the effect of decreasing the electron density in the $2p-\pi$ AOs at the *ortho*- and *para*-carbons and transferring it to the $2p-\pi$ AO on the exocyclic methylene group. The electrostatically favorable transfer of electron density from the benzene ring to exocyclic carbon is what causes the empty $3b_1$ HMO to mix into the filled $2b_1$ HMO.

As shown in Figure 5, this mixing leads to an increase of the exocyclic AO coefficient in $2b_1$, which results in strengthening of the π bond between the CH_2 group and the *ipso*-carbon. In fact, the order of the π bond to the exocyclic carbon increases from 0.635 at the HMO level to 0.794 at the SCF level.¹⁸ This mixing between the HMOs helps to explain the very high barrier to rotation that is computed for the benzyl cation.

The same mixing of the $3b_1$ into the $2b_1$ HMOs also explains the small changes in the bond lengths of the ring of the benzyl cation. The $3b_1$ MO has nodes at the *ipso*- and *meta*-ring carbons, such that the mixing of it into $2b_1$ leaves the coefficients at these carbons unchanged in the $2b_1$ SCF MO. However, the mixing between the HMOs reduces the coefficients at the *ortho*- and *para*-carbons of the $2b_1$ SCF MO and thus weakens the *ortho-ipso* and *meta-para* π bonds. In addition, the small antibonding interaction between the *ortho*- and *meta*-carbons in the $2b_1$ HMO is also diminished in the $2b_1$ SCF MO.

Comparison of the G4 bond lengths in the planar benzyl cation and radical in Figure 3 shows that the bond lengths in the cation differ from those in the radical exactly as expected from consideration of the Coulomb-induced mixing between the $2b_1$ and $3b_1$ Hückel MOs in the cation. Thus, this mixing not only explains why the π bond to the exocyclic carbon is much stronger in the planar benzyl cation than in the radical but also all of the differences in Figure 3 between the calculated C–C bond lengths in the planar benzyl cation and radical.

The same type of mixing between an occupied and empty Hückel MO occurs in the benzyl anion, where in Hückel theory 4/7 of the negative charge is localized at the CH_2 group. As shown in Figure 6, mixing of the empty $4b_1$

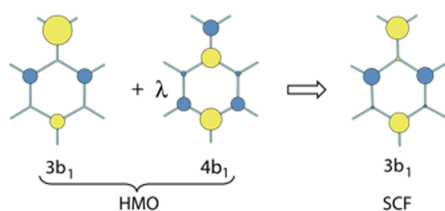


Figure 6. Schematic depiction of the $3b_1$ ($E = \alpha$) and $4b_1$ ($E = \alpha - 1.26\beta$) HMOs of benzyl and the doubly occupied $3b_1$ SCF MO of the anion that results from mixing a small amount ($\lambda < 1$) of the latter HMO into the former HMO.

antibonding MO into the doubly occupied $3b_1$ nonbonding HMO with a positive sign leads to a transfer of electron density from the exocyclic CH_2 group into the benzene ring.¹⁹ This mixing results in the creation, at the *ipso* position, of a small coefficient of the same sign as that on the exocyclic carbon, which creates a bonding π interaction between these two centers. Consequently, in the anion, the order of the π bond to the exocyclic carbon increases from 0.635 at the

HMO level to 0.757 at the SCF level.¹⁸ This increase of 0.122 is, however, slightly smaller than that of 0.159 in the cation (see above), which therefore helps to explain why the rotational barrier in the anion is lower than that in the cation.

The mixing of the $4b_1$ HMO into the $3b_1$ HMO also results in small changes between the radical and the anion in the bond lengths in the benzene ring that are shown in Figure 3. However, none of the C–C bond lengths in the anion are the same as those in the cation. The mixing between the $2b_1$ and $3b_1$ HMOs in the cation appears to have slightly different effects on the C–C bond lengths than the mixing between the $3b_1$ and $4b_1$ HMOs in the anion.

One reason for this difference is that the $3b_1$ HMO is a nonbonding MO, whereas the $4b_1$ HMO contains antibonding π interactions between the *ipso*-carbon and the exocyclic methylene group and between the *meta*- and *para*-carbons. The antibonding interaction between the *ipso*-carbon and the exocyclic methylene group in the $4b_1$ HMO should result in mixing between this HMO and the $3b_1$ HMO in the anion, creating less π bonding between these two carbons than the mixing between $2b_1$ and $3b_1$ in the cation.

An additional factor that distinguishes the anion from the cation is that, when overlap is included, the energy difference between the nonbonding $3b_1$ HMO and the antibonding $4b_1$ HMO is much larger than that between $3b_1$ HMO and the bonding $2b_1$ HMO. The greater energy separation between $4b_1$ and $3b_1$ means that their mixing will be smaller, providing less stabilization than the mixing between $3b_1$ and $2b_1$. This difference between benzyl cation and anion may also help to explain why the G4 barrier to rotation in the benzyl cation is fully 22.0 kcal/mol greater than that in the benzyl anion; for comparison, the barrier to rotation in the allyl cation is only 12.4 kcal/mol greater than that in the allyl anion.

Like the SCF MOs for the benzyl cation and anion, the CASSCF-MOs for the radical are also different from the HMOs. The $3b_1$ CASSCF SOMO of the benzyl radical (see Supporting Information) is more localized on the exocyclic carbon than the $3b_1$ HMO. This partial localization of the SOMO keeps the unpaired electron away from the three π electrons of opposite spin in the benzene ring and thus reduces the Coulombic repulsion between them.

Partially localizing the SOMO of the radical on the exocyclic carbon atom can be achieved by mixing the filled $2b_1$ and the empty $4b_1$ HMO into the $3b_1$ HMO, both with positive signs, which increases the $2p-\pi$ AO coefficient on the exocyclic carbon in the $3b_1$ SOMO. On the other hand, the associated mixing of the $3b_1$ into the $2b_1$ MO with a negative sign results in a shrinking of the AO coefficient on the exocyclic carbon in the $2b_1$ MO, which leads to a decrease in the π bonding to this carbon in the $2b_1$ -MO.

This decrease expresses itself in an attenuation of the π -bond order of the *ipso-exo* bond from 0.635 in HMO theory to 0.427 if the CASSCF MOs are used. This decrease is the cause of the significant lengthening of the bond between the *ipso*- and *exo*-carbons in the benzyl radical compared to the same bond in the cation and the anion, where the MO mixing has the opposite effect (see Figure 3).

The localization of the odd electron on the exocyclic carbon, accompanied by a reduction of the π bonding to that carbon, corresponds to a higher weight of the resonance structure for the benzyl radical where the bond to the exocyclic carbon is a single bond and where the benzene ring is aromatic. This latter feature expresses itself in the much

smaller bond alternation in the ring for the radical than for either of the charged species.

Origin of the Differences between Allyl and Benzyl Cations and Anions. As already noted, the C–C bond lengths in the allyl cation and anion are nearly the same as in the allyl radical, whereas as discussed in the preceding section, the C–C bond lengths are significantly different in benzyl cation and anion from those in the benzyl radical. It would therefore appear that Coulombic effects on π bonding have a much smaller effect in allyl than in benzyl, and this would explain why the barriers to rotation are smaller in the allyl cation and anion than in the benzyl anion and cation.

Although the charge distribution is symmetrical in the allyl cation and anion, it should be the case that delocalization of some of the electron density from the central carbon to the terminal carbons would occur in the allyl cation and that delocalization of the electron density from the terminal carbons to the central carbon would occur in the allyl anion. In MO theory, how would these changes occur in the allyl cation and anion?

In benzyl, the shifts in electron density toward or away from the exocyclic CH_2 group occur by mixing of the nonbonding MO $3b_1$ with the filled $2b_1$ MO in the cation and with the empty $4b_1$ MO in the anion. In both cases, the energy difference in Hückel theory between the filled and empty MOs that mix is 1.26β .

In contrast, at C_{2v} geometries of the allyl, the nonbonding MO has a_2 symmetry, which is different from that of the bonding $1b_1$ π MO and the antibonding $2b_1$ π MO. Therefore, the nonbonding a_2 MO in allyl cannot mix with either the $1b_1$ or the $2b_1$ MO. The only mixing that can affect the distribution of the π electrons in both allyl cation and allyl anion is that between the bonding $1b_1$ π MO and the antibonding $2b_1$ π MO.

However, the Hückel energies of these two MOs differ by 2.82β , which is more than twice the Hückel energy difference of 1.26β between the filled and empty MOs that are mixed in the benzyl anion and cation. The large difference in energy between the MOs that must be mixed to alter the charge distributions in the allyl cation and anion, from those given by Hückel theory, is the reason why the bonding is much less affected by charge in allyl than in benzyl.

As explained above, because the optimal MOs in the benzyl cation, anion, and radical are different from the Hückel orbitals, the HMOs for benzyl cannot be used to perform the same types of PPP calculations that we used to explain the differences between the rotational barriers in the allyl cation, anion, and radical. However, there is every reason to believe that the same types of Coulombic effects that make the rotational barriers in the allyl cation and anion larger than those in the allyl radical also contribute to making the rotational barriers in the benzyl cation and anion larger than those in the benzyl radical.

5. CONCLUSIONS

The rotational barriers of allyl and benzyl cations, radicals, and anions have been calculated with high accuracy quantum chemistry methods including W1BD, G4, and DFT. The barriers of allyl cation, radical, and anion are concluded to be 33, 15, and 21 kcal/mol, respectively. The barriers of benzyl cation, radical, and anion are concluded to be 45, 11, and 24 kcal/mol, respectively. Our computational results show that there is a clear correlation between the rotational barriers and

the resonance stabilization energies measured by isodesmic reactions.

Although the barriers to CH_2 rotation in the allyl cation, radical, and anion are all predicted to be the same at the Hückel level of theory, the reason they are actually quite different from each other has been addressed in detail here. We have analyzed the allyl HMOs and evaluated the most important changes in the electron repulsion energies upon rotation of a CH_2 group. Our calculations show that the changes in Coulombic repulsion between the π electrons that occur on twisting a CH_2 group out of conjugation are responsible for the differences between the barriers to rotation in the allyl cation, radical, and anion.

The changes in Coulombic repulsions that occur on rotating a CH_2 group out of conjugation in the allyl cation, radical, and anion can be summarized as follows: In the allyl cation, the more delocalized bonding MO at the planar geometry makes the mutual Coulombic repulsion energy between the pair of electrons in this MO smaller than that between the pair of electrons in the ethylenic π MO in the twisted geometry. Therefore, a planar geometry is strongly favored by Coulombic effects.

In the allyl radical, two new Coulombic interactions are added, involving the unpaired electron and the pair of electrons in the bonding π MO. The Coulombic repulsion between the unpaired electron and the electron of opposite spin in the bonding MO is smallest when these two electrons are confined to different regions of space, as they are in the twisted geometry of the radical. This is why the barrier to rotation in the allyl radical is smaller than that in the allyl cation.

In the allyl anion, Coulombic repulsions between the bonding and nonbonding pairs of electrons favor the twisted geometry by twice as much as in the radical. However, there is also a new interaction in the anion, the mutual Coulombic repulsion between the two electrons in the nonbonding MO. Because in the twisted geometry both nonbonding electrons are localized in the same AO, this interaction selectively destabilizes the twisted anion by a very large amount of energy, as shown in the last line of Table S2 in the Supporting Information. It is this Coulombic interaction between the two nonbonding electrons in the allyl anion that makes the rotational barrier in the anion higher than that in the allyl radical.

As predicted by HMO theory, the barrier to rotation is slightly smaller in the benzyl radical than in the allyl radical. However, in contrast, the barriers to rotation in the benzyl cation and anion are much larger than those for the same type of ion in allyl.

We show that these dramatic deviations from the predictions of HMO theory are also due to the effects of electron repulsion. These effects result in mixing between filled and unfilled HMOs of the same symmetry. This mixing not only shifts electron density from the benzene ring to the exocyclic carbon in the benzyl cation, and in the opposite direction in the benzyl anion, but this mixing also results in strengthening the π bonding to the exocyclic methylene group in both the anion and cation. The Coulombically induced strengthening of the π bonding to the exocyclic methylene group in benzyl cation and anion are the reason why B^+ and B^- both have higher rotational barriers than those of A^+ and A^- .

Thus, Coulombic effects are responsible for not only the fact that the rotational barriers decrease in the order $A^+ > A^- > A^\bullet$ and $B^+ > B^- > B^\bullet$ but also for the fact that the rotational barriers in B^+ and B^- are greater than those in A^+ and A^- , respectively. HMO theory predicts that the rotational barriers in **A** and **B** should not depend on the number of nonbonding electrons and that the rotational barriers in **B** should all be lower than those in **A**. Only for the relative sizes of the rotational barriers in A^\bullet and B^\bullet does HMO theory make a qualitatively correct prediction.

■ ASSOCIATED CONTENT

📄 Supporting Information

The Supporting Information is available free of charge on the ACS Publications website at DOI: 10.1021/acs.joc.6b01530.

Computational methodologies, experimental conditions, Cartesian coordinates of optimized structures, detailed thermodynamic data, and the results of PPP calculations on the allyl cation, radical, and anion (PDF)

■ AUTHOR INFORMATION

Corresponding Authors

*Email: thomas.bally@unifr.ch.

*Email: houk@chem.ucla.edu.

*Email: borden@unt.edu.

Notes

The authors declare no competing financial interest.

■ ACKNOWLEDGMENTS

We thank the US National Science Foundation (K.N.H., CHE 1059084), the Swiss National Science Foundation (Grant No. 200020_143410), the Natural Science Foundation of China (Z. L., 21002055), the China Scholarship Council (Z. L., 201208110219), and the Robert A. Welch Foundation (W.T.B., Grant B0027) for financial support of this research. Calculations were performed on the Hoffman2 cluster at UCLA and the Extreme Science and Engineering Discovery Environment (XSEDE) supported by the NSF.

■ REFERENCES

- (1) (a) Mayr, H.; Foerner, W.; Schleyer, P. v. R. *J. Am. Chem. Soc.* **1979**, *101*, 6032. (b) Korth, H.-G.; Trill, H.; Sustmann, R. *J. Am. Chem. Soc.* **1981**, *103*, 4483. (c) Thompson, T. B.; Ford, W. T. *J. Am. Chem. Soc.* **1979**, *101*, 5459. (d) Conradi, M. S.; Zeldes, H.; Livingston, R. *J. Phys. Chem.* **1979**, *83*, 2160. (e) Fraenkel, G.; Russell, J. G.; Chen, Y.-H. *J. Am. Chem. Soc.* **1973**, *95*, 3208. (f) Fraenkel, G.; Geckle, J. M. *J. Am. Chem. Soc.* **1980**, *102*, 2869. (g) Mišić, V.; Piech, K.; Bally, T. *J. Am. Chem. Soc.* **2013**, *135*, 8625.
- (2) (a) Dorigo, A. E.; Li, Y.; Houk, K. N. *J. Am. Chem. Soc.* **1989**, *111*, 6942. (b) Wiberg, K. B.; Breneman, C. M.; LePage, T. J. *J. Am. Chem. Soc.* **1990**, *112*, 61. (c) Nicolaidis, A.; Borden, W. T. *J. Am. Chem. Soc.* **1992**, *114*, 8682. (d) Gobbi, A.; Frenking, G. *J. Am. Chem. Soc.* **1994**, *116*, 9275. (e) Hrovat, D. A.; Borden, W. T. *J. Phys. Chem.* **1994**, *98*, 10460. (f) Mo, Y.; Lin, Z.; Wu, W.; Zhang, Q. *J. Phys. Chem.* **1996**, *100*, 6469. (g) Mo, Y. *J. Org. Chem.* **2004**, *69*, 5563. (h) Linares, M.; Humbel, S.; Braida, B. *J. Phys. Chem. A* **2008**, *112*, 13249.
- (3) In HMO theory, α is the energy of an electron in a nonbonding $p\pi$ -AO on carbon, and $\alpha + \beta$ is the energy of the bonding π MO in ethylene. Consequently, α and β both have negative signs. Therefore, the energies for rotations that lead to the disruption of π bonds, which have positive signs, have negative β -values.

(4) The reason why UHF gives a more accurate barrier height than (U)MP2 is discussed in: Bally, T.; Borden, W. T. *Rev. Comput. Chem.* **1999**, *13*, 1.

(5) Courmoyer, M. E.; Jorgensen, W. L. *J. Am. Chem. Soc.* **1984**, *106*, 5104.

(6) Barbour, J. B.; Karty, J. M. *J. Org. Chem.* **2004**, *69*, 648.

(7) (a) Zielinski, M.; Havenith, R. W. A.; Jenneskens, L. W.; van Lenthe, J. H. *Theor. Chem. Acc.* **2010**, *127*, 19. (b) Mo, Y.; Hiberty, P. C.; Schleyer, P. v. R. *Theor. Chem. Acc.* **2010**, *127*, 27.

(8) Frisch, M. J., et al. *Gaussian 03*, revision D.01; Gaussian, Inc.: Wallingford, CT and Pittsburgh, PA, 2004 (complete citation given in the Supporting Information).

(9) Curtiss, L. A.; Redfern, P. C.; Raghavachari, K. *J. Chem. Phys.* **2007**, *126*, 084108.

(10) Barnes, E. C.; Petersson, G. A., Jr.; Montgomery, J. A.; Frisch, M. J.; Martin, J. M. L. *J. Chem. Theory Comput.* **2009**, *5*, 2687.

(11) Marynick, D. S.; Dixon, D. A. *Proc. Natl. Acad. Sci. U. S. A.* **1977**, *74*, 410.

(12) Gobbi, A.; Frenking, G. *J. Am. Chem. Soc.* **1993**, *115*, 2362.

(13) Douberly, G. E.; Ricks, A. M.; Schleyer, P. v. R.; Duncan, M. A. *J. Chem. Phys.* **2008**, *128*, 021102/1.

(14) Ruscic, B. *Active Thermochemical Tables*, version 1.118; Argonne National Laboratories, 2015. Available at <http://atct.anl.gov>.

(15) On the basis of enthalpies of formation from: Afeefy, H. Y.; Liebman, J. F.; Stein, S. E. In *NIST Chemistry WebBook*, NIST Standard Reference Database No 69; Lonstrom, P.J., Mallard, W. G., Eds.; National Institute of Standards and Technology: Gaithersburg, MD, 2005; <http://webbook.nist.gov/chemistry> (accessed in October 2014).

(16) At the UHF level of theory, the electron in the bonding MO of allyl radical that has spin opposite to the unpaired electron in the NBMO tends to localize at the central carbon to minimize the Coulombic repulsion between these two electrons. For complete discussion, see the review cited in ref 4.

(17) (a) Pariser, R.; Parr, R. G. *J. Chem. Phys.* **1953**, *21*, 466. (b) Pople, J. A. *Trans. Faraday Soc.* **1953**, *49*, 1375.

(18) To calculate π -bond orders at the SCF level, the 2p AO coefficients of the π MOs calculated with the STO-3G basis set are normalized to 1 (see listing in the Supporting Information) so that they can be compared to Hückel MOs. Then, the bond orders are calculated as in HMO theory.

(19) If the phase of the AO at the exocyclic carbon in the $3b_1$ and $4b_1$ MOs are chosen to be the same, then these two MOs are mixed with a negative sign in the allyl anion.